First Double Excitation Cross Sections of Helium Measured for 100-keV Proton Impact

P. Moretto-Capelle, D. Bordenave-Montesquieu, and A. Bordenave-Montesquieu
Laboratoire Collisions, Agrégats, Réactivité, IRSAMC, UMR 5589, CNRS and Université Paul Sabatier, 31062 Toulouse Cédex, France

A. L. Godunov* and V. A. Schipakov
Troitsk Institute for Innovation and Fusion Research, Troitsk, Moscow region, 142092, Russia
(Received 25 June 1997)

Excitation cross sections of the $(2s^2)^1S$, $(2p^2)^1D$, and $(2s2p)^1P$ autoionizing states of helium, produced in collisions with 100-keV protons, have been measured for the first time. Using a high resolution electron spectroscopy together with a recently proposed parametrization of autoionizing resonances distorted by Coulomb interaction in the final state makes it possible to extract from electron spectra *total cross sections* as well as *magnetic sublevel populations.* These new experimental data are briefly compared with out theoretical calculations. [S0031-9007(97)04892-8]

PACS numbers: 34.50.Fa

Two-electron excitation of the helium atom by proton impact is currently a benchmark test for the theories of multielectron transitions which try to understand the excitation mechanisms involved in heavy particle collisions [1]. Doubly excited states of helium lie above the single-ionization threshold and decay primarily by autoionization. Since the excitation and subsequent nonradiative decay of autoionizing states is coherent with direct ionization, the resonant and direct ionization amplitudes should be added together, rather than cross sections of both processes [2]. This results in at least two effects. First, the resonances in ionization cross sections are asymmetric. They are commonly described by Fano's formula [2]. Second, the intensity of an autoionizing resonance is not proportional to the population of the resonant state [3]. The total resonant yield can provide only a lower estimate for the excitation cross section at asymptotic collision velocities [4]. This means that information on two-electron excitation is hidden in the resonance profiles. Therefore, comparing the calculation results for two-electron excitation with available experimental data (electron spectra or resonance parameters) requires not only an adequate theoretical description of the double excitation itself, but also a realistic description of the direct ionization, including the interference of resonant and direct ionization. Moreover, Coulomb interaction in the final state (CIFS) between the scattered charged particle, the ejected electron, and the recoil ion considerably influences the resonance profiles [5–8]. Under the conditions of strong CIFS the shapes of the resonant lines can be very different from the familiar Fano's one [5,7] complicating the comparison of experimental and theoretical results, and hence the description of three-body Coulomb interaction of charged particles must be as accurate as the description of two-electron excitation [8]. The theoretical excitation cross sections reported in this paper are part of our complete calculation [8] where all these problems are solved. From another point of view, if we are able to extract excitation cross sections from experimental data instead of resonance yields a comparison with less complex calculations becomes also possible. Indeed, several approximate theoretical models [9–13] have been developed in the past to discuss the excitation mechanisms; they calculated excitation cross sections of doubly excited states considered as bound states; therefore they had not to describe the complex perturbing effects (interference of resonant and direct ionization amplitudes, CIFS). So far it was a common point of view that excitation cross sections of autoionizing states could never be extracted from measured ionization cross sections unless the direct ionization amplitude is small. So the latter theoretical excitation cross sections were considered unrealistic until now since no valid comparison could be made with experiments which measured only resonance yields. However, Godunov *et al.* have recently shown [8,14] that, under conditions of strong enough CIFS, a new parametrization allows a separation of the excitation information from the perturbing effects. The present experimental work is an application of this finding. For the first time, the total excitation cross sections as well as the magnetic sublevel populations of the low-lying autoionizing $(2s^2)^1S$, $(2p^2)^1D$, and $(2s2p)^1P$ states of helium excited by 100-keV proton impact have been extracted from experimental spectra.

This experimental information on the two-electron excitation of autoionizing states by charged particle impact can be extracted from electron spectra under the following conditions: (i) Intermediate collision velocities are studied in order that the influence of CIFS be strong enough to distort the resonant line shapes; (ii) experimental energy resolution is high enough to make apparent such a distortion; (iii) an adequate parametrization of the resonance profiles with allowance for CIFS is used to separate the resonance and interference contributions to the resonant profile; (iv) a measurement of the angular dependence of the electron spectra is performed. All these conditions are satisfied in the present experimental work.

Our study is based on the new parametrization recently proposed [8,14] for the description of resonance profilesin electron emission spectra distorted by CIFS. For the present collision conditions, the doubly differential cross section for electron emission in the vicinity of autoionizing resonances can be written as [8,14]

$$\frac{d^2\sigma}{dE_e d\Omega_e} = F(E_i, E_e, \vartheta_e) + \sum_\mu \frac{\exp(-\xi \arctan \varepsilon_\mu)}{\varepsilon_\mu^2 + 1} \{A_\mu^c(E_i, \vartheta_e) [\varepsilon_\mu \cos(\varphi_\mu(\varepsilon_\mu)) - \sin(\varphi_\mu(\varepsilon_\mu))] + B_{\mathrm{int},\mu}^c(E_i, \vartheta_e) [\cos(\varphi_\mu(\varepsilon_\mu)) + \varepsilon_\mu \sin(\varphi_\mu(\varepsilon_\mu))] + B_{\mathrm{exc},\mu}^c(E_i, \vartheta_e) \exp(-\xi \arctan \varepsilon_\mu)\}, \quad (1)$$

with

$$\xi = \frac{Z_p}{v_f}\left(Z_t - \frac{v_f}{v_{\mathrm{pe}}}\right),$$

$$\varphi_\mu(\varepsilon_\mu) = -\xi \ln(\varepsilon_\mu^2 + 1)/2,$$

where $\varepsilon_\mu = 2(E_e - E_\mu)/T_\mu$ is the relative energy deviation from the resonance position E_μ, E_e is the ejected electron energy, Γ_μ is the resonance width, Z_p and Z_t are the charge of the projectile and the recoil ion accordingly, v_f is the speed of the scattered particle, v_{pe} is the relative speed between the scattered charge particle and the ejected electron. The first term in Eq. (1) is the doubly differential cross section for direct ionization. The new resonant parameters $A_\mu^c(E_i, \vartheta_e)$, $B_{\mathrm{int},\mu}^c(E_i, \vartheta_e)$, and $B_{\mathrm{exc},\mu}^c(E_i, \vartheta_e)$ are given by [8]

$$A_\mu^c(E_i, \vartheta_e) = (2\pi)^4 m_p^2 \frac{K_f k_e}{K_i} 2\mathrm{Re}\left\{K_{\mathrm{res},\mu}^0 \int (t_{\mathrm{dir}}^* t_{\mathrm{dec},\mu} t_{\mathrm{exc},\mu})\, d\Omega_f\right\}, \quad (2)$$

$$B_{\mathrm{int},\mu}^c(E_i, \vartheta_e) = (2\pi)^4 m_p^2 \frac{K_f k_e}{K_i} 2\mathrm{Im}\left\{K_{\mathrm{res},\mu}^0 \int (t_{\mathrm{dir}}^* t_{\mathrm{dec},\mu} t_{\mathrm{exc},\mu}) d\Omega_f\right\}, \quad (3)$$

$$B_{\mathrm{exc},\mu}^c(E_i, \vartheta_e) = (2\pi)^4 m_p^2 \frac{K_f k_e}{K_i} |K_{\mathrm{res},\mu}^0|^2 \int |t_{\mathrm{dec},\mu} t_{\mathrm{exc},\mu}|^2 d\Omega_f, \quad (4)$$

where $\mathbf{K}_i$ and $\mathbf{K}_f$ are the momenta of incident and scattered particles, m_p is the mass of the projectile, $d\Omega_f$ is the solid angle element in the direction of the scattered particle, $K_{\mathrm{res},\mu}^0$ is the electron energy independent part of the kinematic factor allowing for CIFS in the resonant ionization channel, t_{dir} is the amplitude of direct ionization, $t_{\mathrm{exc},\mu}$ and $t_{\mathrm{dec},\mu}$ are the amplitudes for excitation and nonradiative decay of the resonant state μ, respectively. The explicit expressions for the amplitudes and other factors that enter the above equations can be found elsewhere [8,15]. The parameters $A_\mu^c(E_i, \vartheta_e)$ and $B_{\mathrm{int},\mu}^c(E_i, \vartheta_e)$ in Eqs. (2) and (3) reflect the interference of resonant and direct ionization, while the parameter $B_{\mathrm{exc},\mu}^c(E_i, \vartheta_e)$ is the squared absolute value of the resonant amplitudes [Eq. (4)]. Then it is seen from this new parametrization that the influence of CIFS results in the separation of the resonant and interference contributions.

Here, it would be pertinent to indicate the relation of this parametrization [Eq. (1)] to the well known Shore parametrization [16]

$$\frac{d^2\sigma}{dE_e d\Omega_e} = F(E_i, \vartheta_e) + \sum_\mu \frac{A_\mu^s(E_i, \vartheta_e)\varepsilon_\mu + B_\mu^s(E_i, \vartheta_e)}{\varepsilon_\mu^2 + 1}. \quad (5)$$

If the influence of CIFS is weak (large ejection angles or fast collision velocities), the kinematic parameter $\xi \ll 1$, and from Eqs. (1) we obtain [8,14]

$$A_\mu^c(E_i, \vartheta_e) \to A_\mu^S(E_i, \vartheta_e), \quad (6)$$

$$B_{\mathrm{int},\mu}^c(E_i, \vartheta_e) + B_{\mathrm{exc},\mu}^c(E_i, \vartheta_e) \equiv B_\mu^c(E_i, \vartheta_e) \to B_\mu^S(E_i, \vartheta_e). \quad (7)$$

It is easy to see that the information on the excitation of autoionizing states in $B_{\mathrm{exc},\mu}^c(E_i, \vartheta_e)$ is mixed with the interference term $B_{\mathrm{int},\mu}^c(E_i, \vartheta_e)$ in the expression of $B_\mu^S(E_i, \vartheta_e)$, and hence cannot be extracted from experimental spectra when CIFS is weak.

In the absence of the interference terms, with or without CIFS [Eqs. (1) and (5), respectively], extracting the information on the population of the autoionizing states becomes straightforward.

The expression (4) for the resonant parameter $B_{\mathrm{exc},\mu}^c(E_i, \vartheta_e)$ can be presented in a more useful form using the definition for the amplitudes involved [15], namely,

$$\frac{\pi\Gamma_\mu}{2} B_{\mathrm{exc},\mu}^c(E_i, \vartheta_e) \frac{\sinh(\pi\xi)}{\pi\xi} = \sum_{M=-L}^{L} \sigma_{\mathrm{exc}}^{LM}(E_i) P_{LM}^2(\cos(\vartheta_e)), \quad (8)$$

where $P_{LM}(\cos(\vartheta_e))$ is the associated Legendre function and $\sigma_{\mathrm{exc}}^{LM}(E_i)$ designates the excitation cross section for the magnetic sublevel M of the state with total orbital momentum L. The total cross section for the excitation of an autoionizing state is given by

$$\sigma_{\mathrm{exc}}(E_i) = \sum_{M=-L}^{L} \sigma_{\mathrm{exc}}^{LM}(E_i) = (2\pi)^4 m_p^2 \frac{K_f}{K_i} \sum_{M=-L}^{L} \int |t_{\mathrm{exc},\mu}^{LM}|^2 d\Omega_f. \quad (9)$$

The known ϑ_e dependence of the resonant parameter $B_{\mathrm{exc},\mu}^c(E_i, \vartheta_e)$ in (8) has been used to derive the two-electron cross sections $\sigma_{\mathrm{exc}}(E_i)$ and $\sigma_{\mathrm{exc}}^{LM}(E_i)$ by a fitting procedure.

The experimental apparatus used in the present work has been described in detail before [7,8]. Two independent runs have been performed, with energy resolutions of 0.11 and 0.068 eV, respectively, for emission angles between 10° and 160°. These new high-resolution measurements made it possible to resolve the near-lying autoionizing $(2p^2)^1D$ and $(2s2p)^1P$ resonances as well as observe a distortion of the resonance profiles for forward electron emission angles below 40°. Ionization cross sections were put on an absolute scale by a normalization to the direct doubly differential cross section of ionization measured by Rudd *et al.* [18]. We estimate our experimental cross sections to be known within $\pm 35\%$.

The measured profiles of the $(2s^2)^1S$, $(2s2p)^1P$, and $(2p^2)^1D$ resonances have been analyzed using formula (1). A new fitting procedure has been developed for processing the electron emission spectra. For each resonance, the following adjustable parameters have been used: the resonance parameters $A_\mu^c(E_i, \theta_e)$, $B_{\mathrm{int},\mu}^c(E_i, \vartheta_e)$, and the cross sections for double electron excitation $\sigma_{\mathrm{exc}}^{LM}(E_i)$. The resonance position E_μ and width Γ_μ were taken from theoretical calculations. The direct ionization cross section $F(E_i, \theta_e)$ was approximated by a first-order polynomial. Since the excitation cross section $\sigma_{\mathrm{exc}}^{LM}(E_i)$ does not depend on ejection angle, we simultaneously fit spectra measured at different ejection angles; various combinations of spectra were used, each of them defining a fit set; up to a maximum of 15 spectra were fitted together. Using this new fitting procedure strongly restricts the variation of the adjustable parameters. Two additional constraints were used in the fitting procedure: (i) The excitation cross section $\sigma_{\mathrm{exc}}^{LM}(E_i)$ must be positive; (ii) $\sqrt{A_\mu^c(E_i, \theta_e)^2 + B_{\mathrm{int},\mu}^c(E_i, \theta_e)^2} \leq 2\sqrt{B_{\mathrm{exc},\mu}^c(E_i, \theta_e) F(E_i, E_e, \theta_e)}$ where the direct ionization cross section $F(E_i, E_e, \theta_e)$ is determined at the resonance position $E_e = E_\mu$. The latter was simply derived from the definitions of the resonant parameters. The new fitting procedure has been proven to be reliable; it gives stable values of the resonance parameters when different sets of spectra are used. It is worth noting that direct application of Eq. (1) to a single spectrum could be unreliable if the effect of CIFS is comparable with statistical noise.

Examples of fitted electron spectra are presented in Fig. 1 for three ejection angles $\theta_e = 20°$, 90°, and 160° (these spectra are taken from a set of 15 spectra fitted together). The same values of $\sigma_{\mathrm{exc}}^{LM}(E_i)$ are used for all these angles. A good fit can be observed. It is important to note here that Shore's parametrization (5) is unable to fit well the experimental spectra when $\theta_e \leq 40°$ (see also [8]).

The two-electron excitation cross sections $\sigma_{\mathrm{exc}}(E_i)$ together with the relative sublevel populations are presented in Table I. The angular dependence of the expression $[B_{\mathrm{exc},\mu}^c(E_i, \vartheta_e) \frac{\sinh(\pi\xi)}{\pi\xi}]$ [see Eq. (8)] is shown in Fig. 2. The experimental values are averaged over different fit runs; they are compared with our theoretical calculations.

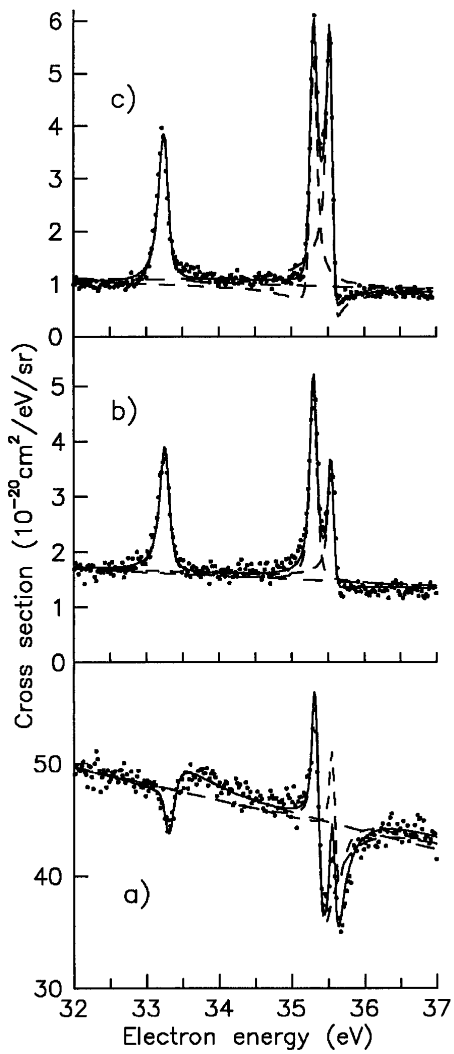

FIG. 1. Experimental electron emission spectra in the region of the $(2s^2)^1S$, $(2p^2)^1D$, and $(2s2p)^1P$ resonances of helium excited by 100-keV proton impact. The energy resolution is equal to 68 meV. The spectra are fitted with formula (1) with inclusion of CIFS (they are part of a set of 15 spectra fitted simultaneously; see text). (a)–(c): angles of emission are equal to 20°, 90°, and 160°, respectively. Experiment: full dots. Results of fit: dotted lines, contribution of each resonance; heavy line, sum of these contributions.

The theoretical model which includes the three-body Coulomb interaction and an expansion of the two-electron excitation amplitudes in powers of the projectile-target interaction up to the second order has been explicitly described earlier [8,15]. Its validity relies on the quantitative agreement achieved between experiment and the calculated electron spectra and resonance parameters $A_\mu^c(E_i, \vartheta_e)$ and $B_\mu^c(E_i, \vartheta_e)$ [8].

A good agreement between theoretical and experimental values for the $(2s2p)^1P$ state can be seen in Table I and Fig. 2 both for total cross section and relative sublevel populations. The magnetic sublevels $M = 0$ and $M = \pm 1$ are about equally populated for $(2s2p)^1P$ and $(2p^2)^1D$ states both in theory and experiment. The weak

TABLE I. Cross sections (in units 10^{-20} cm^2) and sublevel populations (%) for two-electron excitation of the autoionizing $(2s^2)^1S$, $(2p^2)^1D$, and $(2s2p)^1P$ states of helium excited by 100 keV proton impact. Experimental results are presented together with our theoretical calculations.

	Sublevel population			
	$M = 0$	$M = \pm 1$	$M = \pm 2$	$\sigma_{\rm exc}$
$(2s^2)^1S$ expt	1.00			3.40
theor.	1.00			5.97
$(2s2p)^1P$ expt	0.51	0.49		8.80
theor.	0.55	0.45		11.8
$(2p^2)^1D$ expt	0.32	0.57	0.11	9.00
theor.	0.51	0.41	0.08	3.51

populations of the $M = \pm 2$ levels are well reproduced by our theoretical calculations. For the $(2p^2)^1D$ state the discrepancy between experimental and theoretical total cross sections is stronger than for the relative sublevel populations. Such a deviation between calculated and experimental line intensities for this state has also been observed before for intermediate [8] and high-velocity [17] p + He collisions. In a coupled-channel calculation where the doubly excited state is taken as a bound state, Nagy and Bodea [13] recently reported for $\sigma_{\rm exc}(2s2p\ ^1P)$ a value of about 8.2×10^{-20} cm^2 in good agreement with our values in Table I.

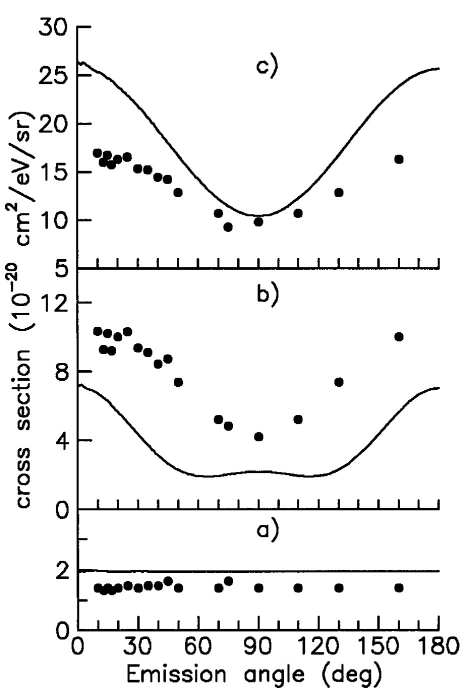

FIG. 2. Angular dependence of the expression $[B^c_{{\rm exc},\mu}(E_i, \vartheta_e)\frac{\sinh(\pi\xi)}{\pi\xi}]$ for the $(2l2l')$ states of helium excited by 100 keV proton impact. (a)–(c): $(2s^2)^1S$, $(2p^2)^1D$, and $(2s2p)^1P$ states, respectively. Present experiment: full dots. Present theory: solid line.

In this paper experimental excitation cross sections of $(2l2l')$ autoionizing states of helium excited by 100 keV proton impact are presented for the first time. Our theoretical calculations are in reasonable agreement with the experimental data. These experimental results provide a deeper insight into the nature of two-electron transitions and become a new challenge for the theory of multiple-electron transitions in ion-atom collisions.

A. G. has appreciated the hospitality of Laboratoire Collisions, Agrégats, Réactivité, IRSAMC, Université Paul Sabatier, Toulouse, France where an important part of the theoretical work has been performed. One of us (A. G.) acknowledges support from the French Ministry of National Education and Scientific Research through Grant No. PECO-CEI n^{0}196547F.

*On leave of absence from Laboratoire Collisions, Agrégats, Réactivité, UMR 5589, IRSAMC, Université Paul Sabatier, 31062 Toulouse Cédex, France.

[1] J. H. McGuire, *Electron Correlation Dynamics in Atomic Collisions* (Cambridge University Press, Cambridge, England, 1997).
[2] U. Fano, Phys. Rev. **124**, 1866 (1961).
[3] T. Åberg and G. Howat, *Theory of the Auger Effect*, Handbuch für Physik, Vol. XXXI, edited by W. Mehlhorn (Springer-Verlag, Berlin, 1982), p. 469.
[4] A. L. Godunov, P. B. Ivanov, and V. A. Schipakov, J. Phys. B **30**, 3403 (1997).
[5] P. W. Arcuni and D. Schneider, Phys. Rev. A **36**, 3059 (1987).
[6] A. L. Godunov, Sh. D. Kunikeev, N. V. Novikov, and V. S. Senashenko, Sov. Phys. JETP **69**, 927 (1989).
[7] P. Moretto-Capelle, M. Benhenni, D. Bordenave-Montesquieu, and A. Bordenave-Montesquieu, J. Phys. B **29**, 2007 (1996).
[8] A. L. Godunov, V. A. Schipakov, P. Moretto-Capelle, D. Bordenave-Montesquieu, M. Benhenni, and A. Bordenave-Montesquieu, J. Phys. B **30**, 5451 (1997).
[9] W. Fritsch and C. D. Lin, Phys. Rev. A **41**, 4776 (1990).
[10] T. G. Winter, Phys. Rev. A **43**, 4727 (1991).
[11] J. C. Straton and J. H. McGuire, Phys. Rev. A **46**, 5514 (1992).
[12] K. Moribayashi, K. I. Hino, and M. Matsuzawa, Phys. Rev. A **46**, 1684 (1992).
[13] L. Nagy and D. Bodea, Nucl. Instrum. Methods Phys. Res., Sect. B **124**, 401 (1997).
[14] A. L. Godunov and V. A. Schipakov, in *Proceedings of the 18th ICPEAC, Aarhus, 1993,* edited by T. Andersen *et al.*, p. 524.
[15] A. L. Godunov, J. H. McGuire, and V. A. Schipakov, J. Phys. B **30**, 3227 (1997).
[16] B. W. Shore, J. Opt. Soc. Am. **57**, 881 (1967).
[17] A. Bordenave-Montesquieu, A. Gleizes, P. Moretto-Capelle, S. Andriamonje, P. Benoit-Cattin, F. Martín, and A. Salin, J. Phys. B **28**, 653 (1995).
[18] M. E. Rudd, L. H. Toburen, and N. Stolterfoht, At. Data Nucl. Data Tables **18**, 413 (1976).